frontiers | Frontiers in Chemistry

TYPE Original Research
PUBLISHED 18 May 2023
DOI 10.3389/fchem.2023.1199921

Check for updates

OPEN ACCESS

EDITED BY
Qidong Hou,
Nankai University, China

REVIEWED BY
Zhiwei Jiang,
Sun Yat-sen University, China
Jingyun Jiang,
Zhengzhou University, China

*CORRESPONDENCE
Xin Huang,
huangxin@cugb.edu.cn

†These authors have contributed equally to this work and share first authorship

RECEIVED 04 April 2023
ACCEPTED 08 May 2023
PUBLISHED 18 May 2023

CITATION
Liu S, Yuan X, Huang X, Huang Y, Sun C, Qian K and Zhang W (2023), Nickel-phytic acid hybrid for highly efficient electrocatalytic upgrading of HMF. *Front. Chem.* 11:1199921. doi: 10.3389/fchem.2023.1199921

COPYRIGHT
© 2023 Liu, Yuan, Huang, Huang, Sun, Qian and Zhang. This is an open-access article distributed under the terms of the Creative Commons Attribution License (CC BY). The use, distribution or reproduction in other forums is permitted, provided the original author(s) and the copyright owner(s) are credited and that the original publication in this journal is cited, in accordance with accepted academic practice. No use, distribution or reproduction is permitted which does not comply with these terms.

Nickel-phytic acid hybrid for highly efficient electrocatalytic upgrading of HMF

Shuyi Liu[1†], Xue Yuan[2†], Xin Huang[2*], Yu Huang[1], Chen Sun[1], Kun Qian[1] and Wenjie Zhang[1]

[1]School of Water Resources and Environment, China University of Geosciences, Beijing, China, [2]School of Science, China University of Geosciences, Beijing, China

Electrocatalytic upgrading of 5-hydroxymethylfurfural (HMF) provides a promising way to obtain both high-value-added biomass-derived chemicals and clean energy. However, development of efficient electrocatalysts for oxidizing HMF with depressed side reactions remains a challenge. Herein, we report a nickel-phytic acid hybrid (Ni-PA) using natural phytic acid as building block for highly efficient electrocatalytic oxidation of HMF to 2, 5-furandicarboxylic acid (FDCA). Due to the coordination of nickel ion and phosphate groups of phytic acid molecule, high selectivity and yield of FDCA were achieved at 1.6 V vs. RHE. Besides, Ni-PA has a higher electrochemical surface area and lower charge-transfer resistance than Cu/Fe-PA, which significantly promotes the oxidation of HMF to FDCA. This work demonstrates the potential of metal-phytic acid hybrids as effective electrocatalysts for biomass valorization.

KEYWORDS

biomass utilization, electrocatalytic oxidation, 5-hydroxymethylfurfural, 2, 5-furandicarboxylic acid, phytic acid

1 Introduction

The increasingly serious environmental pollution and the depletion of fossil fuels have prompted great efforts to develop environment-friendly conversion and clean energy storage technologies (Xie et al., 2018; El-Emam and Özcan, 2019; Mohammed-Ibrahim and Sun, 2019; Haldar and Purkait, 2021). The utilization of abundant and renewable biomass into fine chemicals through direct use of renewable electricity at ambient temperatures and pressures is a significant development direction and has attracted considerable interest (Zhou et al., 2021a; Zheng et al., 2022).5-hydroxymethylfurfural (HMF) is one of the most important biomass platform molecules, which could serve as essential bridge connecting resource to produce industrial chemicals (Lăcătuș et al., 2018; Kong et al., 2020), textiles (Dhivya et al., 2019), and pharmaceutical intermediates (Shao et al., 2022). Over past decades, electrocatalytic oxidation of HMF has attracted much attention due to its obvious advantages of ambient and easily controlled condition compared with aerobic oxidation (Chen C. et al., 2021; Zhao et al., 2021). However, the electrochemical oxidation of HMF still remains a challenge that the competition between water oxidation and HMF oxidation in aqueous media might lead to the decrease of selectivity and yield of FDCA. Thus, many efforts have been made on design of efficient electrodes to improve the HMF conversion efficiency and selectivity of FDCA (Mankar et al., 2019; Pang et al., 2022; Jiang et al., 2023).

In regard of the high cost and undesirable catalytic performance of noble metals, transition metal compounds (Ni, Fe, Co, and Mn) have been widely used as electrodes for

electrocatalytic oxidation of HMF and showed high FDCA yield and Faradaic efficiency in recent years (Taitt et al., 2018; Cai et al., 2020; Bai et al., 2021; Zhang et al., 2021; Jing et al., 2023; Li et al., 2023; Lie et al., 2023). Ni-based materials show extremely high catalytic activity, which far exceeds that of other transition metals or metal alloys (Lu et al., 2020; Zhou et al., 2021b; Gao et al., 2022; Wu et al., 2022; Xu et al., 2022).The main reason is that Ni element has the abundant three-dimensional electron number and the unique, e.g., orbitals, which could enhance the covalency of the transition metal and oxygen bonds (Formenti et al., 2018; Dutta et al., 2019). Grabowski et al. (Grabowski et al., 1991)first reported the use of NiO/$Ni(OH)_2$ for the electrocatalytic oxidation of HMF, and the FDCA yield was only 71%. Subsequently, various Ni-based compounds, such as nitrides (Zhang et al., 2019; Chen W. et al., 2021), phosphides (Lu et al., 2021), sulfides (Wang W. et al., 2021), borides (Barwe et al., 2018), oxides (Choi et al., 2020; Wang J. et al., 2021), hydroxides (Zhang et al., 2021), layered double hydroxides (LDHs) (Zhongming et al., 2021) and their composites, have been wildly investigated to electro-oxidation of HMF and demonstrated a high FDCA yield and FE. Despite these strategies developed for electrooxidation of HMF over nickel-based catalysts, designing of advanced materials and achieving high current densities at low potentials remains challenging.

The application of biomass-based material from renewable natural compounds is of great significance since the diversity of natural compounds provides unlimited possibilities and potential for designing abundant functional materials (Vinod et al., 2020; Zhang et al., 2022). Phytic acid ($C_6H_{18}O_{24}P_6$), for example, as a natural organic macromolecule distilled from grain, can coordinate with multiple metal ions and form strong bonds due to the presence of six phosphate groups and twelve hydroxyl groups in its structure (He et al., 2022). At that point, functional materials derived from phytic acid have shown great advantages and promising prospects in many fields, including coatings (Li et al., 2022; Song et al., 2022), catalysis (Wang et al., 2018; Gwóźdź and Brzęczek-Szafran, 2022; Song et al., 2023; Yang et al., 2023), and pharmaceuticals (Wang Y. et al., 2021). Herein, we prepared metal-phytic acid hybrids using natural phytic acid as building block, and Ni-phytic acid hybrid (Ni-PA) shows high catalytic performance in the electrochemical oxidation of HMF. The active Ni ion chelated with phytic acid to form nanomaterial with pore structure. It has high electrochemical active surface area and low charge transfer resistance. As a result, the Ni-PA catalyst exhibits outstanding performance for the oxidation of HMF to FDCA with high yield of 99.1% and FE for FDCA (90%) at 1.6 V vs. RHE.

2 Experimental section

2.1 Materials and methods

Anhydrous $NiCl_2$ was purchased from Thermo Fisher Scientific, Anhydrous $FeCl_3$, Anhydrous $CuCl_2$, 5-hydroxymethylfurfural (HMF) and sodium phytate were purchased from Adamas, Nafion D-521 dispersion, Toray Carbon Paper (CP, TGP-H-60, 19 × 19 cm), Nafion N-117 membrane were purchased from Alfa Aesar China Co., Ltd. potassium hydroxide and potassium chloride were purchased from General-reagent. All reagents from commercial sources were used without further purification.

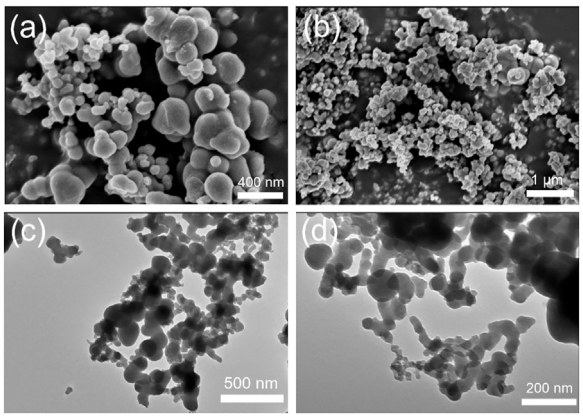

FIGURE 1
Characterizations of the prepared Ni-PA. **(A) (B)** SEM images, **(C) (D)** TEM images.

2.2 Synthesis of metal-PA

Synthesis of Ni-PA: In a typical synthesis, sodium phytate (5 mmol) and $NiCl_2$ (15 mmol) were dissolved in deionized water (300 mL). The mixture was stirred at room temperature for 2 h and then aged in static conditions at room temperature for 12 h. Finally, the light green precipitate was separated by centrifugation and dried in the oven at 50 °C for 12 h.

Synthesis of Fe-PA and Cu-PA: The synthetic process of Fe-PA and Cu-PA is similar to Ni-PA except that the precursor $NiCl_2$ is replaced by 15 mmol $FeCl_3$ or $CuCl_2$, respectively.

2.3 Catalyst characterization

The scanning electron microscopy (SEM) measurements were performed using a Hitachi S-4800 scanning electron microscope operated at 15 kV. Transmission electron microscopy (TEM) images were obtained from a JEOL-1011 resolution transmission electron microscopy. Powder X-ray diffraction (XRD) patterns were obtained on the X-ray diffractometer (Model D/MAX2500, Rigaka) with Cu-Kα radiation. X-ray photoelectron spectroscopy (XPS) analysis was performed on the Thermo Scientific ESCA Lab 250Xi using 200 W monochromatic Al Kα radiation, and the 500 μm X-ray spot was used. The base pressure in the analysis chamber was about 3×10^{-10} mbar. Typically, the hydrocarbon C1s line at 284.8 eV from adventitious carbon was used for energy referencing.

2.4 Electrochemical experiment

Preparation of electrode: 5 mg of the as-prepared materials and 10 μL of Nafion D-521 dispersion were dispersed in 1 mL absolute ethyl alcohol to create a homogeneous suspension by sonication.

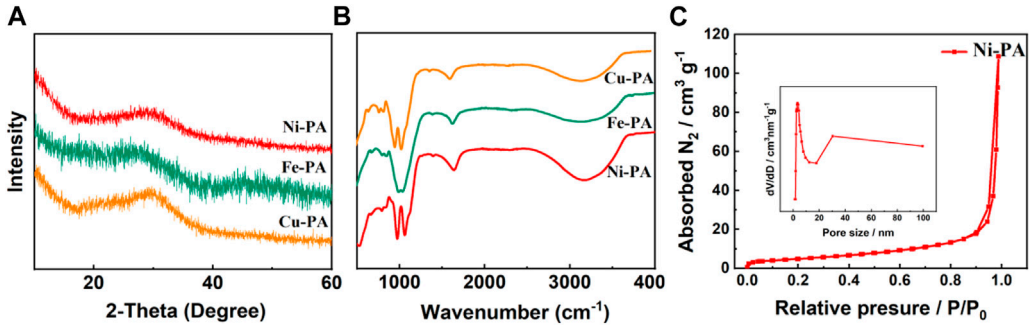

FIGURE 2
(A) XRD, **(B)** FTIR patterns of metal-phytic acid hybrids, **(C)** N_2 adsorption–desorption isotherm and pore size distribution of Ni-PA.

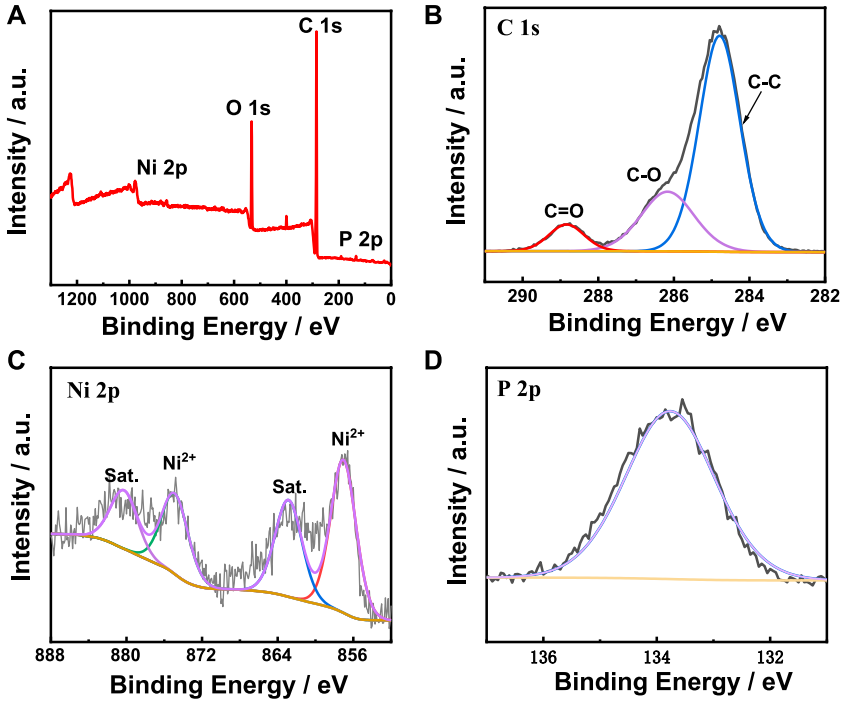

FIGURE 3
XPS spectra of Ni-PA catalyst. **(A)** full-scan spectrum, **(B)** C 1s, **(C)** Ni 2p, and **(D)** P 2p spectra.

The suspension was then dripped on carbon paper (CP, 1 cm × cm). After drying in air, a catalyst with the loading of 5 mg cm^{-2} was obtained based on the weight change of the CP.

Linear sweep voltammetry (LSV) measurements: LSV measurements were performed using an electrochemical workstation (CHI 760E, Shanghai Chenhua Instrument Co., Ltd.). And typical H-type electrolytic cell was used, which is separated by a Nafion N-117 membrane. The H-type electrolysis cell contained three electrodes, including a working electrode, a platinum grid counter electrode, and an Ag/AgCl reference electrode. In addition, the anolyte electrolyte and catholyte electrolyte were 1 M KOH aqueous solution. LSV measurements were carried out under mild magnetic stirring, with a potential range of 1.0–2.0 V vs. RHE and a scanning speed of 10 mV/s.

Electrochemical oxidation of HMF: Electrochemical performance of the materials was assessed with a CHI 760 electrochemical workstation using a typical H-type cell at room temperature. The H-type electrolytic cell was divided into anode and cathode chambers with a Nafion N-117 proton exchange membrane. By the calculation of 0.197 + 0.059× pH, all potentials were converted from vs. Ag/AgCl to vs. RHE. The electrochemical oxidation experiment was performed in a 1.0 M KOH solution of 15 mL with or without 10 mM HMF.

3 Results and discussion

The prepared metal-phytic acid hybrids were first characterized by scanning electron microscopy (SEM) and transmission electron

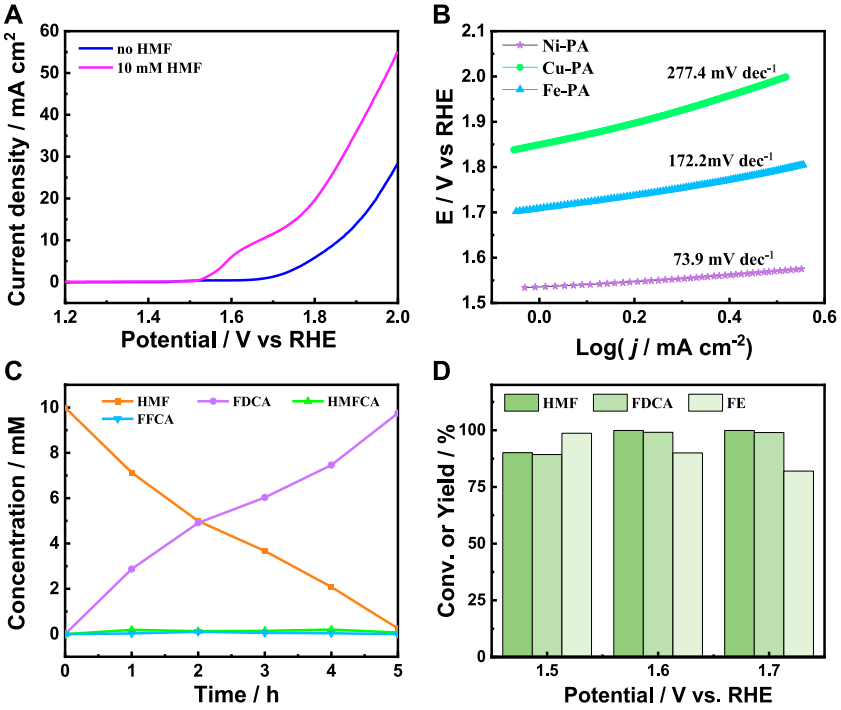

FIGURE 4
(A) LSV curves of Ni-PA with and without HMF at a scan rate of 0.1 V/s in 1.0 M aqueous KOH solution, **(B)** Tafel plots of metal-phytic acid hybrids with HMF, **(C)** Concentrations of HMF and the oxidation products during electrolysis, and **(D)** The HMF conversion, yield and FE of FDCA at different applied potentials over Ni-PA.

microscopy (TEM), and the morphology results are shown in Figure 1, Supplementary Figure S2 and S3. The SEM and TEM images of Ni-PA show that it has an irregular tubular and spherical shape (Figure 1). The diameter of the sphere is about 100–200 nm, and the length of irregular strip is between 200 and 300 nm with the width of about 100 nm. The Cu-PA catalyst shows similar morphology as Ni-PA, while the deformation of the tube is more serious (Supplementary Figure S1). And the Fe-PA consists of small particles with the diameter of about 40 nm (Supplementary Figure S2).

The XRD patterns of various metal-phytic acid hybrids were shown in Figure 2A, which all exhibited the same structure characteristics. The results showed that all the metal-phytic acid hybrids were poorly ordered and amorphous, indicating the nanoparticles in metal-phytic acid hybrids are arranged irregularly, which is consistent with the SEM results (Song et al., 2015). Flourier transform infrared spectroscopy (FTIR) spectroscopy was then performed to research the chemical structures of metal-phytic acid hybrids samples (Figure 2B), and the peaks at 3400 cm^{-1} and 1642 cm^{-1} are corresponded to the absorbed H_2O. The peak at 1063 cm^{-1} could be assigned to the Ni-O-P stretching vibrations, which clearly demonstrates the formation of coordination bond of Ni^{2+} ions and phosphate ester group (Xue et al., 2016; Xie et al., 2020). N_2 adsorption–desorption isotherm and pore size distribution of Ni-PA in Figure 2C show that the catalyst has a typical microporous structure. The surface area and pore diameter are 64.1 m^2/g and 0.71 nm, respectively. Cu-PA shows similar N_2 adsorption–desorption isotherm with that of Ni-PA, while Fe-PA shows a typical mesoporous structure with the surface area of 125.8 m^2/g and a pore diameter of 17.4 nm (Supplementary Figure S3 and Supplementary Table S1).

2Moreover, the X-ray photoelectron spectroscopy (XPS) was carried out to analyze the electronic states and element composition of metal-phytic acid hybrids. The XPS spectrum of Ni-PA in Figure 3A shows that Ni-PA is mainly composed of C, O, P and Ni. For C 1s spectrum of Ni-PA, the peak can be fitted into three peaks at 284.8, 286.2 and 288.8 eV, corresponding to C-C, C-O and C=O (Figure 3B). The Ni 2p XPS spectrum of Ni-PA in Figure 3C shows the Ni $2p_{1/2}$ and Ni $2p_{3/2}$ binding energies at 874.7 and 857.0 eV, respectively, indicating the existence of Ni^{2+} in Ni-PA. The peak of P 2p (Figure 3D) at 133.8 eV corresponds to phytic acid. For O 1s (Supplementary Figure S4), two peaks at 532.1 eV and 533.5 eV could be obtained by peak split, and which corresponds to the C-O and C=O. The XPS spectra of Cu-PA and Fe-PA catalysts in Supplementary Figure S5 demonstrate that the catalysts consist of C, O, P, Cu and C, O, P, Fe, respectively. These results indicate that Ni/Cu/Fe element has been successfully coordinated with phytic acid.

The electrocatalytic performance of HMF oxidation over metal-phytic acid hybrids was firstly investigated by linear sweep voltammetry (LSV) in 1.0 M KOH electrolyte. Figure 4A present the LSV curves of Ni-PA with and without 10 mM HMF,

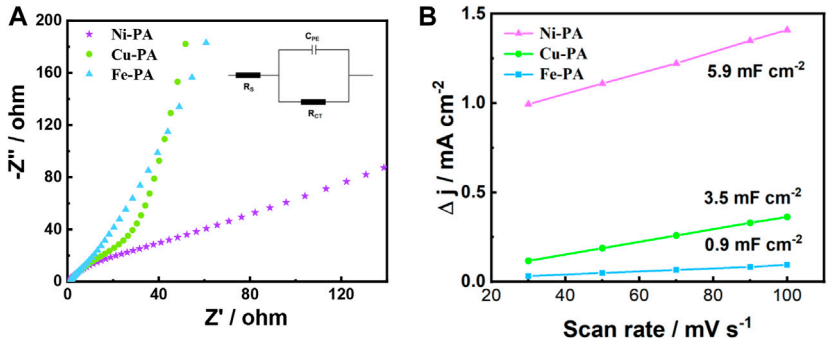

FIGURE 5
(A) Nyquist plots (inside is the equivalent circuit of electrochemical impedance spectroscopy), and **(B)** Charging current density differences plotted against scan rates of various metal-phytic acid electrodes in 1.0 M KOH solution.

respectively, and the oxidation peak at 1.67 V is associated with the oxidation of Ni^{2+} to higher oxidation state (Xu et al., 2022). The onset potential shifted from 1.64 V to 1.50 V after adding 10 mM HMF, and the current density increased dramatically with 10 mM HMF, indicating that the oxidation of HMF was more favorable than water oxidation. Besides, as shown in Figure 4A and Supplementary Figure S6, Ni-PA possessed the highest current density and a lowest current density onset potential among the metal-phytic acid hybrids, indicating Ni-PA was more active to the HMF oxidation than Cu-PA and Fe-PA. The Tafel slope of Ni-PA with HMF was calculated as 73.9 mV dec^{-1} (Figure 4B), much lower than that of Cu-PA (277.4 mV dec^{-1}) and Fe-PA (172.2 mV dec^{-1}), indicating a much faster catalytic kinetics of Ni-PA at the anode after adding HMF. Based on these results, the constant potential electrolysis of HMF was conducted over Ni-PA in 1.0 M KOH electrolyte at an applied potential of 1.6 V vs. RHE. High-performance liquid chromatography (HPLC) was used to obtain the concentration of HMF and oxidation products. As can be seen from Figure 4C, the concentration of HMF decreased and the amount of FDCA increased with the extension of reaction time, indicating that HMF was successfully oxidized to FDCA. In addition, there is a small amount of 5-hydroxymethyl-2-furanocarboxylic acid (HMFCA) and 2-formyl-5-furanocarboxylic acid (FFCA) could be detected during the reaction time, which have been reported as common reaction intermediates in the electrolysis of HMF to FDCA (Fu et al., 2022). After 5 h electrolysis at 1.6 V, HMF could be completely converted to FDCA, and the yield and Faraday efficiency of FDCA could reach 99.1% and 90%, respectively. Moreover, Ni-PA exhibited better HMFOR activity compared to other reported electrocatalysts (Supplementary Table S2). The applied potential also affects the HMF oxidation results. As shown in Figure 4D, the yield of FDCA increases with the increase of applied potential, while the Faraday efficiency decreases with the increase of applied potential. Considering both the FDCA yield and Faraday efficiency of the reaction, the most suitable potential in our catalytic system is 1.6 V vs. RHE. In addition, Ni-PA showed a superior yield of FDCA compared with Cu-PA and Fe-PA (Supplementary Figure S7), indicating the superior activity of Ni-PA for HMF oxidation to FDCA. The durability test of Ni-PA was then conducted through five electrolysis. As shown in Supplementary Figure S8, there was no significant decrease in the yield and FE of FDCA. The Ni-PA recovered after five times reuses was then characterized by XPS, FT-IR, XRD, SEM and TEM (Supplementary Figure S9, S10), and no notable difference could be found, indicating the good cyclic stability.

To investigate the reason for the excellent performance of the Ni-PA on the electro-oxidation of HMF to FDCA, electrochemical impedance spectroscopy (EIS) and cyclic voltammetry (CV) measurements were performed to investigate the electrode/electrolyte interface properties of various metal-phytic acid electrodes. The Nyquist plots of various metal-phytic acid electrodes were shown in Figure 5A. In which Ni-PA performed the lowest charge transfer resistance (Rct) of 1.8 Ω, much smaller than that of Cu-PA (3.9 Ω) and Fe-PA (4.2 Ω), respectively, indicating a more facile electron transfer process and faster reaction rate. Besides, the electrochemical surface area (ECSA) results obtained from the double-layer capacitance in CV curves against scan rates (Supplementary Figure S11) are shown in Figure 5B. It is obvious that Ni-PA possess the maximum slope of 5.9 mF cm^{-2} among various metal-phytic acid electrodes, thus has a highest electrochemical active surface area. It indicates that there are more reactive sites in Ni-PA for HMF, probably driving from the coordination of Ni and phytic acid.

4 Conclusion

In summary, various metal-phytic acid hybrids (Ni-PA, Fe-PA, Cu-PA) have been successfully synthesized by precipitation method. The prepared catalysts were investigated to electrochemical oxidation of HMF and Ni-PA showed excellent activity to produce FDCA. The yield and Faradaic efficiency of FDCA could reach 99.1% and 90% respectively at an applied potential of 1.6 V vs. RHE, much higher than that of Fe-PA and Cu-PA. Electrochemical tests show that Ni-PA has high electrochemical surface area and low charge transfer resistance, which enhanced the activity and selectivity for the

electrochemical oxidation of HMF to FDCA. We believe that this work provides an efficient strategy to explore the biomass resources to prepare functional materials, which may have great application in the field of catalysis.

Data availability statement

The original contributions presented in the study are included in the article/Supplementary Material, further inquiries can be directed to the corresponding author.

Author contributions

SL, YH, CS, KQ, and WZ: Experimental operation and data collection; XY: Experimental data collection and analysis; XH: Data analysis and article writing. All authors contributed to the article and approved the submitted version.

Funding

This work was financially supported by College Student Innovation and Entrepreneurship Training Program, China University of Geosciences (Beijing), and Fundamental Research Funds for the Central Universities (Grant No. 2-9-2021-009).

Conflict of interest

The authors declare that the research was conducted in the absence of any commercial or financial relationships that could be construed as a potential conflict of interest.

Publisher's note

All claims expressed in this article are solely those of the authors and do not necessarily represent those of their affiliated organizations, or those of the publisher, the editors and the reviewers. Any product that may be evaluated in this article, or claim that may be made by its manufacturer, is not guaranteed or endorsed by the publisher.

Supplementary material

The Supplementary Material for this article can be found online at: https://www.frontiersin.org/articles/10.3389/fchem.2023.1199921/full#supplementary-material

References

Bai, X.-J., He, W.-X., Lu, X.-Y., Fu, Y., and Qi, W. (2021). Electrochemical oxidation of 5-hydroxymethylfurfural on ternary metal–organic framework nanoarrays: Enhancement from electronic structure modulation. *J. Mat. Chem. A* 9, 14270–14275. doi:10.1039/D1TA02464G

Barwe, S., Weidner, J., Cychy, S., Morales, D. M., Dieckhöfer, S., Hiltrop, D., et al. (2018). Electrocatalytic oxidation of 5-(hydroxymethyl) furfural using high-surface-area nickel boride. *Angew. Chem. Int. Ed.* 57, 11460–11464. doi:10.1002/anie.201806298

Cai, M., Zhang, Y., Zhao, Y., Liu, Q., Li, Y., and Li, G. (2020). Two-dimensional metal–organic framework nanosheets for highly efficient electrocatalytic biomass 5-(hydroxymethyl) furfural (HMF) valorization. *J. Mat. Chem. A* 8, 20386–20392. doi:10.1039/D0TA07793C

Chen, C., Wang, L., Zhu, B., Zhou, Z., El-Hout, S. I., Yang, J., et al. (2021a). 2, 5-Furandicarboxylic acid production via catalytic oxidation of 5-hydroxymethylfurfural: Catalysts, processes and reaction mechanism. *J. Energy Chem.* 54, 528–554. doi:10.1016/j.jechem.2020.05.068

Chen, W., Xie, C., Wang, Y., Zou, Y., Dong, C., Huang, Y., et al. (2021b). Activity origins and design principles of nickel-based catalysts for nucleophile electrooxidation. *J. Energy Chem.* 61, 2974–2993. doi:10.1016/j.chempr.2020.07.022

Choi, S., Balamurugan, M., Lee, K.-G., Cho, K. H., Park, S., Seo, H., et al. (2020). Mechanistic investigation of biomass oxidation using nickel oxide nanoparticles in a CO_2-saturated electrolyte for paired electrolysis. *J. Phys. Chem. Lett.* 11, 2941–2948. doi:10.1021/acs.jpclett.0c00425

Dhivya, E., Magadevan, D., Palguna, Y., Mishra, T., and Aman, N. (2019). Synthesis of titanium based hetero MOF photocatalyst for reduction of Cr (VI) from wastewater. *J. Environ. Eng.* 7, 103240. doi:10.1016/j.jece.2019.103240

Dutta, S., Iris, K., Tsang, D. C., Ng, Y. H., Ok, Y. S., Sherwood, J., et al. (2019). Green synthesis of gamma-valerolactone (gvl) through hydrogenation of biomass-derived levulinic acid using non-noble metal catalysts: A critical review. *Chem. Eng. J.* 372, 992–1006. doi:10.1016/j.cej.2019.04.199

El-Emam, R. S., and Özcan, H. (2019). Comprehensive review on the techno-economics of sustainable large-scale clean hydrogen production. *J. Clean. Prod.* 220, 593–609. doi:10.1016/j.jclepro.2019.01.309

Formenti, D., Ferretti, F., Scharnagl, F. K., and Beller, M. (2018). Reduction of nitro compounds using 3d-non-noble metal catalysts. *Chem. Rev.* 119, 2611–2680. doi:10.1021/acs.chemrev.8b00547

Fu, M., Yang, W., Yang, C., Zhang, Y., and Shen, C. (2022). Mechanistic insights into CoO_x–Ag/CeO_2 catalysts for the aerobic oxidation of 5-hydroxymethylfurfural to 2, 5-furandicarboxylic acid. *Catal. Sci. Technol.* 12, 116–123. doi:10.1039/D1CY01599K

Gao, L., Wen, X., Liu, S., Qu, D., Ma, Y., Feng, J., et al. (2022). Nickel-vanadium-cobalt ternary layered double hydroxide for efficient electrocatalytic upgrading of 5-hydroxymethylfurfural to 2, 5-furancarboxylic acid at low potential. *J. Mat. Chem. A* 10, 21135–21141. doi:10.1039/D2TA03016K

Grabowski, G., Lewkowski, J., and Skowroński, R. (1991). The electrochemical oxidation of 5-hydroxymethylfurfural with the nickel oxide/hydroxide electrode. *Electrochim. Acta* 36, 1995. doi:10.1016/0013-4686(91)85084-K

Gwóźdź, M., and Brzęczek-Szafran, A. (2022). Carbon-based electrocatalyst design with phytic acid—a versatile biomass-derived modifier of functional materials. *Int. J. Mol. Sci.* 23, 11282. doi:10.3390/ijms231911282

Haldar, D., and Purkait, M. K. (2021). A review on the environment-friendly emerging techniques for pretreatment of lignocellulosic biomass: Mechanistic insight and advancements. *Chemosphere* 264, 128523. doi:10.1016/j.chemosphere.2020.128523

He, X., Zhang, J., Xie, L., Sathishkumar, G., Li, C., Rao, X., et al. (2022). Phytic Acid-Promoted rapid fabrication of natural polypeptide coatings for multifunctional applications. *Chem. Eng.* 440, 135917. doi:10.1016/j.cej.2022.135917

Jiang, Z., Zeng, Y., Hu, D., Guo, R., Yan, K., and Luque, R. (2023). Chemical transformations of 5-hydroxymethylfurfural into highly added value products: Present and future. *Green Chem.* 25, 871–892. doi:10.1039/D2GC03444A

Jing, T., Yang, S., Feng, Y., Li, T., Zuo, Y., and Rao, D. (2023). Selective and effective oxidation of 5-hydroxymethylfurfural by tuning the intermediates adsorption on Co-Cu-CN_x. *Nano Res.* 2023, 1–9. doi:10.1007/s12274-023-5450-3

Kong, Q.-S., Li, X.-L., Xu, H.-J., and Fu, Y. (2020). Conversion of 5-hydroxymethylfurfural to chemicals: A review of catalytic routes and product applications. *Fuel Process Technol.* 209, 106528. doi:10.1016/j.fuproc.2020.106528

Lăcătuș, M., Bencze, L., Toșa, M., Paizs, C., and Irimie, F. (2018). Eco-friendly enzymatic production of 2, 5-bis (hydroxymethyl) furan fatty acid diesters, potential biodiesel additives. *ACS Sustain. Chem. Eng.* 6, 11353–11359. doi:10.1021/acssuschemeng.8b01206

Li, L., Qi, P., Peng, A., Sun, J., Cui, Z., Liu, W., et al. (2022). Preparation of durable flame retardant nylon-cotton blend fabrics by 3-glycidyloxypropyl trimethoxy silane associated with polyethyleneimine and phytic acid. *Cellulose* 29, 7413–7430. doi:10.1007/s10570-022-04693-5

Li, S., Wang, S., Wang, Y., He, J., Li, K., Xu, Y., et al. (2023). Doped Mn enhanced NiS electrooxidation performance of HMF into FDCA at industrial-level current density. *Adv. Funct. Mat.* 2023, 2214488. doi:10.1002/adfm.202214488

Lie, W. H., Yang, Y., Yuwono, J. A., Tsounis, C., Zubair, M., Wright, J., et al. (2023). Identification of catalytic activity descriptors for selective 5-hydroxymethyl furfural

electrooxidation to 2, 5-furandicarboxylic acid. *J. Mat. Chem. A* 11, 5527–5539. doi:10.1039/D2TA08306J

Lu, X., Wu, K. H., Zhang, B., Chen, J., Li, F., Su, B. J., et al. (2021). Highly efficient electro-reforming of 5-hydroxymethylfurfural on vertically oriented nickel nanosheet/carbon hybrid catalysts: Structure–function relationships. *Angew. Chem. Int. Ed.* 133, 14649–14656. doi:10.1002/ange.202102359

Lu, Y., Dong, C.-L., Huang, Y.-C., Zou, Y., Liu, Y., Li, Y., et al. (2020). Hierarchically nanostructured NiO-Co $_3$ O $_4$ with rich interface defects for the electro-oxidation of 5-hydroxymethylfurfural. *Sci. China Chem.* 63, 980–986. doi:10.1007/s11426-020-9749-8

Mankar, S. V., Garcia Gonzalez, M. N., Warlin, N., Valsange, N. G., Rehnberg, N., Lundmark, S., et al. (2019). Synthesis, life cycle assessment, and polymerization of a vanillin-based spirocyclic diol toward polyesters with increased glass-transition temperature. *ACS Sustain. Chem. Eng.* 7, 19090–19103. doi:10.1021/acssuschemeng.9b04930

Mohammed-Ibrahim, J., and Sun, X. (2019). Recent progress on Earth abundant electrocatalysts for hydrogen evolution reaction (HER) in alkaline medium to achieve efficient water splitting–A review. *J. Energy Chem.* 34, 111–160. doi:10.1016/j.jechem.2018.09.016

Pang, X., Bai, H., Zhao, H., Fan, W., and Shi, W. (2022). Efficient electrocatalytic oxidation of 5-hydroxymethylfurfural coupled with 4-nitrophenol hydrogenation in a water system. *Acs Catal.* 12, 1545–1557. doi:10.1021/acscatal.1c04880

Shao, Y., Wang, J., Sun, K., Gao, G., Fan, M., Li, C., et al. (2022). Cu-based nanoparticles as catalysts for selective hydrogenation of biomass-derived 5-hydroxymethylfurfural to 1, 2-hexanediol. *ACS Appl. Nano Mat.* 5, 5882–5894. doi:10.1021/acsanm.2c01077

Song, F., Zhao, Q., Zhu, T., Bo, C., Zhang, M., Hu, L., et al. (2022). Biobased coating derived from fish scale protein and phytic acid for flame-retardant cotton fabrics. *Mat. Des.* 221, 110925. doi:10.1016/j.matdes.2022.110925

Song, J., Hua, M., Huang, X., Ma, J., Xie, C., and Han, B. (2023). Robust bio-derived polyoxometalate hybrid for selective aerobic oxidation of benzylic C (sp^3)–H bonds. *Acs Catal.* 13, 4142–4154. doi:10.1021/acscatal.2c05519

Song, J., Zhou, B., Zhou, H., Wu, L., Meng, Q., Liu, Z., et al. (2015). Porous zirconium–phytic acid hybrid: A highly efficient catalyst for meerwein–ponndorf–verley reductions. *Angew. Chem.* 54, 9399–9403. doi:10.1002/anie.201504001

Taitt, B. J., Nam, D.-H., and Choi, K.-S. (2018). A comparative study of nickel, cobalt, and iron oxyhydroxide anodes for the electrochemical oxidation of 5-hydroxymethylfurfural to 2, 5-furandicarboxylic acid. *Acs Catal.* 9, 660–670. doi:10.1021/acscatal.8b04003

Vinod, A., Sanjay, M., Suchart, S., and Jyotishkumar, P. (2020). Renewable and sustainable biobased materials: An assessment on biofibers, biofilms, biopolymers and biocomposites. *J. Clean. Prod.* 258, 120978. doi:10.1016/j.jclepro.2020.120978

Wang, J., Zhao, Z., Shen, C., Liu, H., Pang, X., Gao, M., et al. (2021a). Ni/NiO heterostructures encapsulated in oxygen-doped graphene as multifunctional electrocatalysts for the HER, UOR and HMF oxidation reaction. *Catal. Sci. Technol.* 11, 2480–2490. doi:10.1039/D0CY02333G

Wang, S., Nam, G., Li, P., Jang, H., Wang, J., Kim, M. G., et al. (2018). Highly active bifunctional oxygen electrocatalysts derived from nickel–or cobalt–phytic acid xerogel for zinc–air batteries. *Nanoscale* 10, 15834–15841. doi:10.1039/C8NR04733B

Wang, W., Kong, F., Zhang, Z., Yang, L., and Wang, M. (2021b). Sulfidation of nickel foam with enhanced electrocatalytic oxidation of 5-hydroxymethylfurfural to 2, 5-furandicarboxylic acid. *Dalton Trans.* 50, 10922–10927. doi:10.1039/D1DT02025K

Wang, Y., Zhang, X., Cao, J., Huang, X., and Zhang, X. (2021c). Multifunctional E-textiles based on biological phytic acid-doped polyaniline/protein fabric nanocomposites. *Adv. Mat. Technol.* 6, 2100003. doi:10.1002/admt.202100003

Wu, J., Kong, Z., Li, Y., Lu, Y., Zhou, P., Wang, H., et al. (2022). Unveiling the adsorption behavior and redox properties of PtNi nanowire for biomass-derived molecules electrooxidation. *ACS Nano* 16, 21518–21526. doi:10.1021/acsnano.2c10327

Xie, C., Song, J., Hua, M., Hu, Y., Huang, X., Wu, H., et al. (2020). Ambient-temperature synthesis of primary amines via reductive amination of carbonyl compounds. *Acs Catal.* 10, 7763–7772. doi:10.1021/acscatal.0c01872

Xie, C., Song, J., Wu, H., Hu, Y., Liu, H., Yang, Y., et al. (2018). Naturally occurring gallic acid derived multifunctional porous polymers for highly efficient CO_2 conversion and I_2 capture. *Green Chem.* 20, 4655–4661. doi:10.1039/C8GC02685H

Xu, X., Song, X., Liu, X., Wang, H., Hu, Y., Xia, J., et al. (2022). A highly efficient nickel phosphate electrocatalyst for the oxidation of 5-hydroxymethylfurfural to 2, 5-furandicarboxylic acid. *ACS Sustain. Chem. Eng.* 10, 5538–5547. doi:10.1021/acssuschemeng.2c00121

Xue, Z., Zhang, Y., Li, G., Wang, J., Zhao, W., and Mu, T. (2016). Niobium phytate prepared from phytic acid and NbCl 5: A highly efficient and heterogeneous acid catalyst. *Catal. Sci. Technol.* 6, 1070–1076. doi:10.1039/C5CY01123J

Yang, D., Chen, M., and Yang, J.-H. (2023). Porous dehydroxyl cobalt phytate as electrocatalyst for high-efficiency water oxidation. *Appl. Surf. Sci.* 609, 155405. doi:10.1016/j.apsusc.2022.155405

Zhang, J., Gong, W., Yin, H., Wang, D., Zhang, Y., Zhang, H., et al. (2021). *In situ* growth of ultrathin Ni (OH) $_2$ nanosheets as catalyst for electrocatalytic oxidation reactions. *ChemSusChem* 14, 2935–2942. doi:10.1002/cssc.202100811

Zhang, N., Zou, Y., Tao, L., Chen, W., Zhou, L., Liu, Z., et al. (2019). Electrochemical oxidation of 5-hydroxymethylfurfural on nickel nitride/carbon nanosheets: Reaction pathway determined by *in situ* sum frequency generation vibrational spectroscopy. *Angew. Chem. Int. Ed.* 131, 16042–16050. doi:10.1002/ange.201908722

Zhang, W., Zhang, P., Wang, H., Li, J., and Dai, S. Y. (2022). Design of biomass-based renewable materials for environmental remediation. *Trends Biotechnol* 40, 1519–1534. doi:10.1016/j.tibtech.2022.09.011

Zhao, Y., Cai, M., Xian, J., Sun, Y., and Li, G. (2021). Recent advances in the electrocatalytic synthesis of 2, 5-furandicarboxylic acid from 5-(hydroxymethyl) furfural. *J. Mat. Chem. A* 9, 20164–20183. doi:10.1039/D1TA04981J

Zheng, L., Zhao, Y., Xu, P., Lv, Z., Shi, X., and Zheng, H. (2022). Biomass upgrading coupled with H 2 production via a nonprecious and versatile Cu-doped nickel nanotube electrocatalyst. *J. Mat. Chem. A* 10, 10181–10191. doi:10.1039/D2TA00579D

Zhongming, Z., Linong, L., Xiaona, Y., Wangqiang, Z., and Wei, L. (2021). Ultrathin layered double hydroxides nanosheets array towards efficient electrooxidation of 5-hydroxymethylfurfural coupled with hydrogen generation. *Appl. Catal. B* 2021. doi:10.1016/j.apcatb.2021.120669

Zhou, B., Dong, C.-L., Huang, Y.-C., Zhang, N., Wu, Y., Lu, Y., et al. (2021a). Activity origin and alkalinity effect of electrocatalytic biomass oxidation on nickel nitride. *J. Energy Chem.* 61, 179–185. doi:10.1016/j.jechem.2021.02.026

Zhou, B., Li, Y., Zou, Y., Chen, W., Zhou, W., Song, M., et al. (2021b). Platinum modulates redox properties and 5-hydroxymethylfurfural adsorption kinetics of Ni (OH) $_2$ for biomass upgrading. *Angew. Chem. Int. Ed.* 60, 22908–22914. doi:10.1002/anie.202109211